Hardness and Structure of Electrodeposited Nickel From a Nickel Sulfamate-Formamide Bath

By V.B. Singh and R.S. Sarabi

The influence of various factors, such as current density, bath and annealing temperatures, on microhardness of electrodeposited nickel from a nickel sulfamate-formamide bath was investigated. Bright, adherent, fine-grained and almost defect-free nickel deposits with moderately high hardness were obtained at 50 °C and a current density of 0.6 A/dm². The microhardness of the nickel deposits decreased with an increase in annealing temperature. The effect of annealing at various temperatures on structure of the deposits was also studied. Recrystallization of grains and grain growth in the deposits were clearly observed at high annealing temperatures. The structural and crystallographic features of the deposits were examined by SEM, TEM and X-ray diffraction studies. Hydrogen content of the deposits was also determined. The structure and hardness showed correlation with hydrogen content in the deposits.

Electrodeposition of metals from aqueous solutions is limited by the discharge potential of hydrogen. Consequently, the main impetus for electrodeposition studies in non-aqueous solvents is the need to obtain electrodeposits of metals that have a more electronegative discharge potential than hydrogen. In electrodeposition from aqueous media, hydrogen evolution reduces the efficiency of deposition of metals and affects the hardness, ductility, brittleness, and microstructure of the deposits. It has been established that as the amount of hydrogen codeposited with the coating decreases, microhardness is lowered.[1,2] Hydrogen codeposition causes displacement of metal atoms from their normal sites, and the resulting crystal lattice distortions give rise to a series of physico-mechanical property changes, as well as to the structure of the deposit. The larger size and different nature of the organic solvent molecules offer a variety of ion solvation probabilities; the deposits may have some very different and desirable mechanical properties compared with deposits from aqueous systems. Consequently, electrodeposition of metals from non-aqueous baths[3-5] seemed promising, and indeed proved quite responsive, emerging as a good alternative to aqueous solutions.

Bath Composition and Conditions

Parameters	Values
Nickel sulfamate, $Ni(SO_3NH_2)_2 \cdot 2H_2O$	0.4 M
Boric acid	0.2 M
Current density	0.4–2 A/dm²
Bath temperature	20–80 °C
Duration of electrolysis	30 min
Agitation	none
Cathode current efficiency	84–93%
Thickness of deposits	3.1–11.5 μm

Many investigators have discussed the role of hydrogen in the structure and properties of electrodeposits.[6,7] The effects of hydrogen inclusion in nickel deposits have aroused much interest. The possibility of a high rate of deposition and formation of a deposit with low internal stress and high hardness[8] are some advantages offered through use of a nickel sulfamate electrolyte. Because of this, a systematic investigation of electrodeposition of nickel from a non-aqueous solvent (formamide) was undertaken. The physical properties and structure of the deposits were studied under various experimental conditions for the effects of hydrogen.

Experimental Procedure

The same procedures were followed as described in earlier work.[9] Typical bath compositions and conditions are given in the table. The plating solution was prepared by dissolving the required amounts of nickel sulfamate and boric acid in purified formamide. A glass cell containing 250 mL of the plating solution was used for deposition. A mechanically polished, scratch-free rectangular copper sheet (2 x 1 x 0.01 cm) degreased and pickled, was used as a cathode by placing

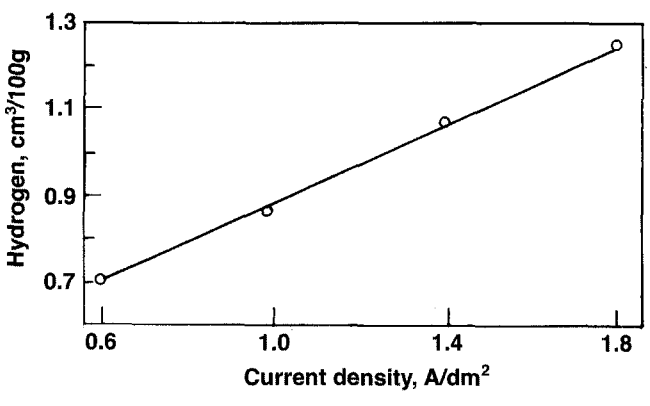

Fig. 1—Variation with current density of hydrogen content of deposits.

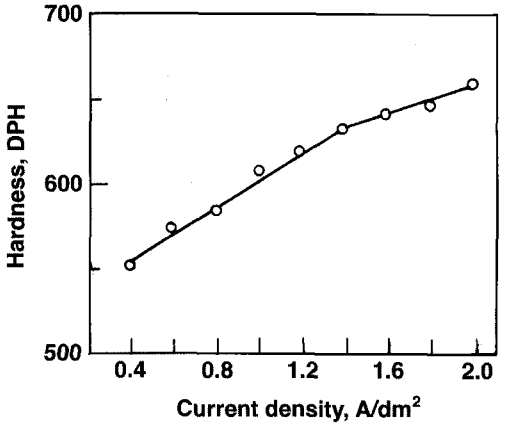

Fig. 2—Effect of current density on microhardness (0.4 M nickel sulfamate and 0.2 M boric acid).

impurities in the deposit is not distinct, it can be concluded from the presence of numerous peaks that the direction of crystal orientation is different for the two deposits. The assorted orientations of the crystal may be the reason for the dullness of the deposit obtained from Bath B. The *hkl* values and average lattice parameters are shown in Table 8.

Findings

1. The Hull Cell patterns of the deposit from the electrochemically prepared bath differ from the commercial, as a result of impurities in the commercial bath. Under identical conditions, the current efficiency for the deposition and throwing power of the electrolyte prepared by electrochemical method is better than that obtained with the commercial electrolyte.
2. The deposits obtained from the electrochemically prepared tin fluoborate are less porous, more easily solderable and more corrosion resistant than those from the commercial bath.
3. The SEM photomicrographs show that the deposits from the electrochemically prepared fluoborate bath are more compact than those obtained from the commercial bath.

Editor's note: *Manuscript received, March 1996.*

References

1. J.W. Mellor, *A Comprehensive Treatise on Inorganic and Theoretical Chemistry,* Longmans Green & Co., New York, NY, 1964; Vol. 6, p. 128.
2. A.L. Ferguson, U.S. patent 2,457,798 (1949), *CA* **43**, 2745 (1949).
3. Andre Riesser, French patent 1,199,639 (1959), *CA* **55**, 9810 (1961).
4. Ullmanns, *Encyclopedia of Industrial Chemistry,* 5th Ed. p. 313-14, Elevers S. Hawkins and G. Schulz, New York (1991).
5. Kirk-Othmer, *Encyclopedia of Chemical Technology,* 3rd Ed., **23**, Wiley Interscience, New York, NY, 1983; p.490.
6. F.A. Lowenheim, *Modern Electroplating,* 3rd Ed., John Wiley & Sons, Inc., New York, NY, 1966.
7. J.P. Langres, *Plat. and Surf. Fin.,* **70**, 21 (Jan. 1983).
8. S.M. Silaimani, M. Pushpavanam and K.C. Narasimham, unpublished data.
9. V.E. Carter, *Metallic Coatings for Corrosion Control,* Newness, Butterworths, London, 1977.
10. R. Sard, O. Oglinn and S. Leidheiser, *Symp. Electrochem. Soc.,* (1974).
11. ASTM Standards 02-05 B537 (1985).
12. M. Stern and A.C. Geary, *J. Electrochem. Soc.,* **104**, 56 (1957).
13. ASTM Standards, 02-05 B545 (1985).

Silaimani

Pushpavanam

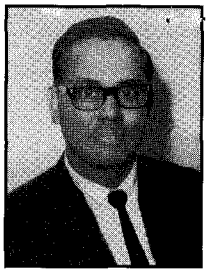

Narasimham

About the Authors

Dr. S.M. Silaimani is a research fellow/associate in the Industrial Metal Finishing Division of the Central Electrochemical Research Institute (CECRI), Karaikudi 630 006, Tamilnadu, India. She has published 10 papers in the area of metal finishing.

Dr. Malathy Pushpavanam is a researcher at the Central Electrochemical Research Institute. She has published more than 170 papers and holds 15 patents in metal finishing.

Dr. K.C. Narasimham is working as scientist emeritus at CECRI, having retired as deputy director and head of the Electrochemicals Division. He has published more than 150 research papers. He also holds 26 patents and has won five awards for developed processes.

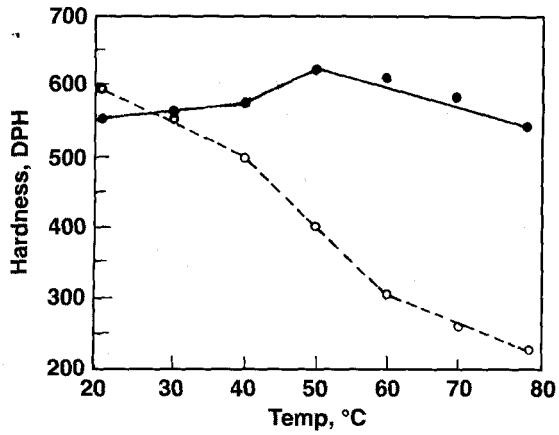

Fig. 3—•—• Variation of microhardness with bath temperature (0.4 M Nickel sulfamate, 0.2 M boric acid and CD 0.6 A/dm²); o—o annealing temperature (for deposits obtained at 50 °C. Temperature scale is x 10 for dotted line curve).

it between two parallel pieces of sulfur-depolarized electrolytic nickel anodes. The interelectrode distance was 2 cm and the cell was thermostatically controlled.

All experiments were performed without agitation and for 30 min duration. The microhardness tests of the deposit surfaces were performed using a microhardness tester with a 136-degree Vickers diamond pyramid indenter and 25-g load. Each hardness value in this report is the average of several measurements. The nickel-plated specimens were vacuum-sealed in a glass tube and annealed at various temperatures 200 to 800 °C for two hr, then allowed to cool slowly to room temperature. The specimens for the TEM studies were prepared by thinning the as-deposited nickel by electropolishing, as reported earlier.[10] Microstructure of nickel deposits was examined using SEM and TEM; X-ray diffraction used CuKα radiation and accelerating voltages of 10, 30, and 100 kV at 20 mA. Hydrogen content was determined by the hot extraction method.

Results and Discussion

Hydrogen Determination

It was found that the hydrogen content of the nickel deposits increased with increasing current density (Fig. 1). Hydrogen codeposition at optimum current density (0.6 A/dm²) was 0.7163 cm³/100 g, but 1.2591 cm³/100 g at the high current density of 1.8 A/dm². The amount of hydrogen inclusion was observed to be very low, compared with a reported aqueous bath.[11] It is known that crystal defects increase with increasing hydrogen content, but codeposition in these studies was low, therefore its effects on crystal growth, physico-mechanical properties and deposit structure were expected to be minimal.

Effect of Current Density, Bath and Annealing Temperature

Bright, adherent and fine-grained deposits, free of pits and cracks were obtained at 50 °C and current density of 0.6 A/dm². Microhardness was found to increase regularly from 555 to 660 DPH with increase in current density (Fig. 2). Such increase is attributed to progressive grain refinement; this trend being similar to that usually reported in the literature.[12,13]

Physico-mechanical properties are also affected by the nature of the solvent used for electrolysis. The protic nature of formamide probably allows a layer of nickel to contain hydrogen as a hydride, which also contributes to hardness to some extent. It can be seen from Fig. 3 that with increasing bath temperature, microhardness increases up to 50 °C (from 553 to 622 DPH) and declines thereafter to 543 at 80 °C. It appears that 50 °C is the most suitable temperature for obtaining hard deposits (622 DPH), because conditions are favorable for formation of basic colloidal hydroxide, which may yield harder deposits.[7]

The influence of the annealing temperature (200 to 800 °C) on microhardness of the as-deposited nickel, obtained under optimum conditions, was investigated. The results are shown in Fig. 3. Measurements showed more or less continuous decrease as the annealing temperature increased. Different temperature ranges revealed different magnitudes of variation; for example, the decrease in hardness in the range of 400 to 600 °C is more significant than in the lower and higher ranges. Such trends can be considered as indications of the occurrence of different physical phenomena in these ranges. It is likely that the deposits in the lower range resulted in relief of internal microstresses that may have existed in the deposits because of cold working.

The deposits became increasingly softer and more ductile with elevated temperature. This may be ascribed mainly to recrystallization and partly to escape of some occluded hydrogen. During recrystallization, new grains form and residual stress is practically eliminated; therefore, considerable decrease in hardness could be observed between 400 and 600 °C. Above 600 °C, because grain growth appears complete, leading to abnormal growth, there is a relatively slow decrease in hardness. Such variation with annealing temperature has been reported earlier for nickel deposits from both aqueous[14] and non-aqueous[15] solutions.

SEM Studies

SEM studies showed the formation of fine-grained deposits with nearly lamellar structure that were produced at 50 °C and current density of 0.6 A/dm², as is evident from the micrograph of Fig. 4a. Nakahara and Felder[11] reported that inclusion of basic colloidal salts influences the microstructure of electrodeposited nickel and that these inclusions are likely to be trapped during growth steps in film formation. Inhibition of growth is thought to be responsible for fine-grained deposits. A remarkable alteration in the microstructure of the deposits was observed when subjected to annealing; the characteristic

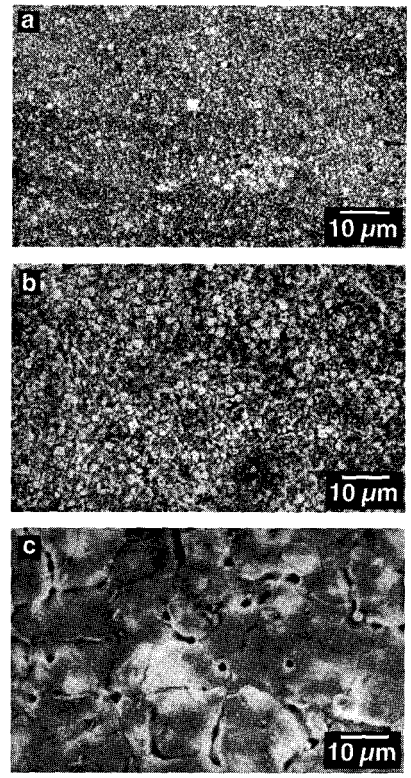

Fig. 4—SEM micrographs of electrodeposited nickel: (a) deposits obtained under optimum conditions (0.4 M nickel sulfamate, 0.2 M boric acid, CD 0.6 A/dm² at 50 °C); (b) & (c) deposits obtained under optimum conditions and subjected to annealing temperature at 400 °C (b) and 800 °C (c), respectively.

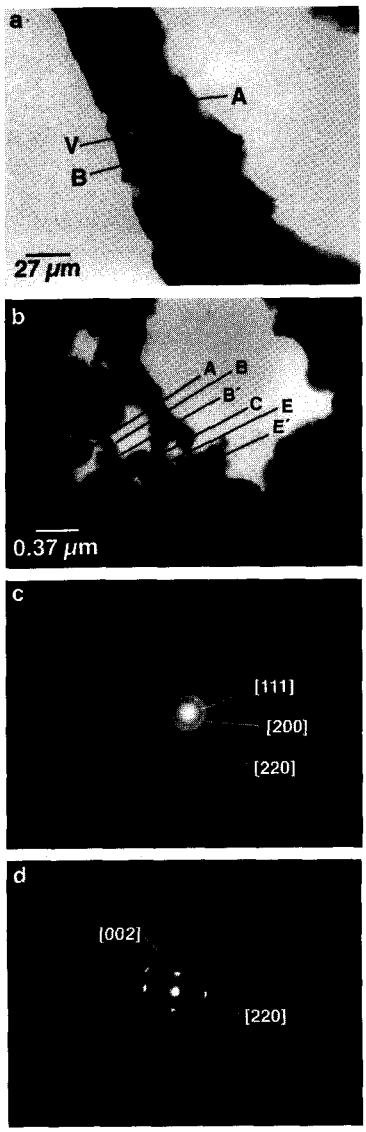

Fig. 5—TEM micrographs of electrodeposited nickel: (a) & (b) bright field image, CD 0.6 A/dm²; (c) & (d) SAD pattern, CD 0.6 A/dm².

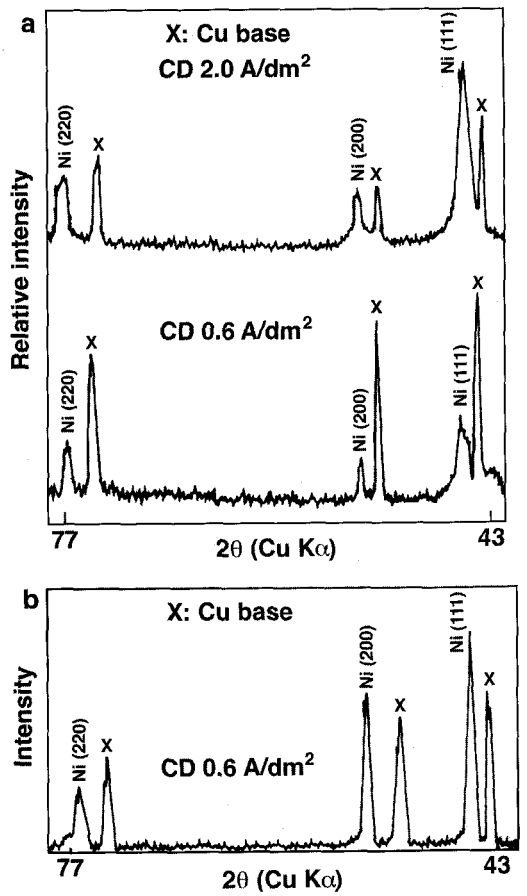

Fig. 6—X-ray diffraction patterns of as-deposited nickel film at different current densities: (a) before annealing; (b) after annealing at 800 °C only at optimum current density.

features can be identified from the SEM micrographs (Figs. 4b-c).

Distinct change in the microstructure is not noticeable when annealed at 200 °C, but at 300 °C, definite change can be observed. The fine cells grow to well-shaped subgrains; also, large numbers of recrystallized nuclei grow rapidly. At 400 °C, the structural features reveal that the deposits are almost recrystallized with homogeneous equiaxed grains (Fig. 4b). The recrystallization process appears complete at 600 °C, but was followed by abnormal grain growth at 700 and 800 °C (Fig. 4c). This figure clearly indicates the presence of pores along the grain boundaries. These pores may have developed as a result of escaping hydrogen, or from any other non-metallic inclusion upon annealing.

TEM and X-ray Diffraction Studies

Electropolished specimens of the as-deposited nickel, obtained under optimum conditions, were subjected to TEM inspection for microstructural and crystallographic characteristics. Figures 5a-b and 5c-d are the TEM micrographs representing the bright field image and selected area diffraction (SAD) patterns of the deposits, respectively. Figure 5a represents the grain distinguished from the diffraction around A and B. The slowly varying contrast throughout the region suggests grain texturing with preferred orientation. The region of the deposit contains several voids; a typical void is outlined V and around V. They may contain hydrogen and could be an internal source of stress. Another microstructural feature can be identified (Fig. 5b) by two grains, indicated around A and C and the grain boundary BB′. Another feature of the deposit is that it is in the form of elliptical precipitates, two of which are marked by E and E′. These precipitates and voids have been reported to play a significant role in modifying the annealing characteristics.[16] The overall interpretation for Figs. 5a-b is that the deposits are free of any type of dislocations, twinning and stacking faults. Such faults have been reported, however, for electrodeposits, from aqueous sulfamate solutions, that also exhibited preferred orientation under certain conditions.[17,18] The development of crystal defects such as dislocations and twins may result from the formation and subsequent coalescence of crystallites. These defects determine the mechanical properties.

Figure 5c corresponds to a ring diffraction pattern. The first two lines represent electron diffraction, showing the polycrystalline nature of the deposit. The first two lines outward from the origin have the indices [111] and [200]. The next (third) line has the index [220]. As can be seen in the third diffraction ring, the pattern does not represent complete randomization of the crystallites, but shows a rather discontinuous nature. These features suggest texturing of the nickel grain. It can be seen that the texturing feature has also been outlined in the microstructural pattern of Fig. 5a. Here, slowly varying contrast between neighboring grains suggests texturing of the grain.

Figure 5d shows SAD from a single grain. In this case, the spots are arranged on a nearly rectangular grid. The index of the spot corresponding to the longer side is [220], that of the shorter side is [002]. The similar SAD patterns obtained from neighboring grains suggest that the preferred orientation is along <120>. The broad microstructural characteristics emerging are representative of a typical fcc lattice of nickel and preferred orientation of the grain in this system.

X-ray diffraction analysis of the as-deposited nickel at different current densities indicates the development of a slight preferred orientation of grains along [220] at the optimum current density of 0.6 A/dm²; also at 2 A/dm² (selected patterns only, shown in Fig. 6a). This can be observed from the intensity of the Ni [220] plane, which is slightly higher than that of the Ni [200] plane at both current densities. According to the standard intensity ratio, the intensity of the Ni [220] plane must be lower than that of the [200] plane. The fcc structure of the nickel deposits was confirmed by X-ray diffraction, which yielded the lattice constant 3.325 Å, in close agreement with the literature.

Defects and texture formation in nickel deposits are commonly observed in deposition from aqueous solutions,[11,19] and they are significantly affected by the plating conditions. Preferred orientation is considered the result of slow growth

of crystalline facets because of inhibition; adsorption of hydrogen or other foreign materials can modify the growth rate. Preferred orientation is known to become increasingly predominant in nickel deposits as the current density increases, and as texture formation influences the brightness, electrical contact resistance and corrosion resistance.[20] A change in preferred orientation in nickel deposits from the [100] plane to [210], with increased hydrogen permeation, with increasing current density, has been reported.[21] In the present bath, the nature, physical properties and structure of the deposits suggest that the inhibiting effect caused either by hydrogen or other species, does not appear dominant, because the deposits are almost free of defects.

The X-ray diffraction studies, after annealing at 800 °C (Fig. 6b), revealed that there was only minor rearrangement in the microstructure. The deposit, which was slightly oriented preferentially along the Ni [220] plane (Fig. 6a) prior to annealing, became randomly oriented along the same plane after annealing. Such minor structural rearrangement may be attributed to the probable escape of hydrogen and by annealing only at high temperature.

Conclusions

An overall examination of the experimental results indicates that the organic, non-aqueous bath may find applications in producing bright, adherent, moderately hard, fine-grained, and almost defect-free nickel deposits. In this study, the hardness of the deposits decreased with increasing annealing temperature. X-ray diffraction revealed only a slight preferred orientation in the nickel deposits, which are randomly oriented when subjected to high annealing temperature. The results also reveal that hydrogen inclusion and its consequent structural implications can be effectively prevented if deposition is from a non-aqueous bath.

Editor's note: *Manuscript received, April 1996; revision received, July 1996.*

Acknowledgments

The authors wish to thank Prof. R.I. Gupta, head of the Dept. of Chemistry, for providing the necessary facilities. Financial support from UCG, New Delhi, is also acknowledged.

References

1. A. Janko and A. Szummer, *Bull. Acad. Pol. Sci.*, **14**, 885 (1966).
2. E.M. Levy, R.D. McInnis and T.P. Copps, *Plating*, **56**, 533 (May 1969).
3. T. Takei, *Electrochim. Acta*, **25**, 1231 (1980).
4. A.A. Sarabi and V.B. Singh, *J. Electrochem. Soc.*, **136**, 2950 (1989).
5. V.B. Singh and R. Sadeghi Sarabi, *Surf. Eng.*, **9**, 156 (1993).
6. Ling Yong, *J. Electrochem. Soc.*, **97**, 241 (1950).
7. S. Nakahara and S. Mahajan, *ibid.*, **127**, 283 (1980).
8. M.M. Rahman and P.K. Tikoo, *Mater. Trans., JIM*, **30**, 530 (1989).
9. P.K. Tikoo, V.B. Singh and S. Sultan, *Plat. and Surf. Fin.*, **71**, 64 (July 1984).
10. S. Kaja, H.W. Pickering and W.R. Bitler, *Plat. and Surf. Fin.*, **73**, 58 (Jan. 1986).
11. S. Nakahara and E.C. Felder, *J. Electrochem. Soc.*, **129**, 45 (1982).
12. R. Weil and H.J. Read, *Metal Fin.*, **53**(12), 60 (1955); **54**(1), 56 (1956).
13. A.T. Vagramyan and Yu.S. Petrova, "The Mechanical Properties of Electrolytic Deposits," Consultants Bureau, New York, NY (1960); p. 90.
14. B.E. Jacobson and J.W. Sliwa, *Plat. and Surf. Fin.*, **66**, 42 (Sept. 1979).
15. V.B. Singh and R. Sadeghi Sarabi, *Mat. Sci. Technol.*, **11**(3), 317 (1995).
16. C.Y. Mak, S. Nakahara, Y. Okinaka, H.S. Trap and J.A. Taylor, *J. Electrochem. Soc.*, **140**, 2363 (1993).
17. S.K. Werma and H. Wilman, *J. Phys. D.*, **4**, 2051 (1971).
18. S. Kaja, H.W. Pickering and W.R. Bitler, *Plat. and Surf. Fin.*, **73**, 58 (Jan. 1986).
19. R. Weil, *Plat. and Surf. Fin.*, **74**, 70 (Dec. 1987).
20. S.L. Ng and Hung. C. Ling, *J. Electrochem. Soc.*, **137**, 458 (1990).
21. W. Paatsch, *Plat. and Surf. Fin.*, **75**, 52 (Aug. 1988).

About the Authors

Dr. V.B. Singh is a reader in physical chemistry in the Dept. of Physical Chemistry, Banaras Hindu University, Varanasi 221 005, India. He is engaged in corrosion studies and electrodeposition of metals and alloys in organic solvents and has published 60 papers in this area. He holds MSc and PhD degrees in chemistry from Banaras Hindu University.

Dr. R.S. Sarabi is employed by a petroleum organization in Iran. He was awarded a PhD in chemistry from Banaras Hindu University in 1995. He has published several research papers on electrodeposition of nickel.

N-Heterocyclic Organic Compounds as Additives For A-C Electrolytic Coloring of Anodized Aluminum From Nickel Sulfate Solutions Part II. Mechanism of Their Action

By B. Karagianni, I. Tsangaraki-Kaplanoglou

In this study, an attempt was made to investigate the mechanism of the action of piperidine-4-carboxylic acid in comparison with piperidine-3-carboxylic acid during a-c electrolytic coloring of anodized aluminum in nickel sulfate-boric acid solution. Electrochemical impedance spectroscopy (EIS) data were used, as well as some other electrochemical techniques. Conformations of the additives that influence action between the opposite charges seem to play a significant role. They are correlated with the ability of the additive to be adsorbed on the electrode surface despite the alternating current, to interfere in the re-anodizing process, and in the nickel deposition rate and distribution.

In Part I of our study,[1] several N-heterocyclic compounds were used as additives during the electrolytic coloring of anodized aluminum from nickel sulfate solutions. It was recognized that some of them improve the throwing power (TP) and/or the color intensity of the probes when added to the coloring baths in certain ranges of concentration. This effectiveness was correlated with their aromatic or saturated character, the position of their characteristic groups and the number of carbon atoms in their rings.

The best influence on the color intensity of the probes was observed in the case of piperidine-4-carboxylic acid, which also improves the TP. It is interesting, therefore, to study in more detail its mode of action and to compare it with that of piperidine-3-carboxylic acid, which has the same positive influence on TP, but not on color intensity. For this reason, electrochemical impedance spectroscopy (EIS) has been used to characterize the surface of electrolytically colored anodized aluminum, during the earlier stages of the a-c coloring treatment, with the presence of the above additives at a higher voltage. EIS is a new technique in development and has been already used to elucidate the process of sealing[2-4] and to clarify a-c electrolytic coloring theoretically.[5-7] In this study, an attempt will be made to gain new information about the effect of these two additives on the anodized aluminum surface, and to elucidate their role during a-c electrolytic coloring in nickel sulfate baths.

Other instrumentation, such as the oscillograph, was also used in the present study for some electrical characteristics of the barrier layer to be measured. They were compared with those from EIS for the proposed mechanism, according to the EIS data,[8,9] to be confirmed.

Experimental Procedure

Test specimens of 1050 aluminum alloy foil with dimensions 2 x 4 x 0.1 cm were used. The surface of the specimen was covered with araldite (epoxy resin), except for a unit area of 10.7 cm^2. The samples were pre-treated, anodized, and electrolytically colored, as in Part I.[1] The electrolytic coloring baths contained:

The reference solution T (30 g/L $NiSO_4 \cdot 6H_2O$ and 30 g/L H_3BO_3)

Solution A (solution T plus 0.07 g/L piperidine-4-carboxylic acid)

Solution B (solution T plus 0.07 g/L piperidine-3-carboxylic acid)

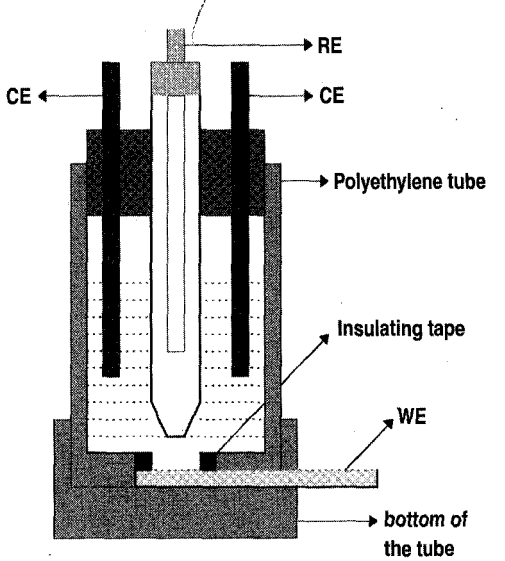

Fig. 1—Cross section of test cell. RE - Reference Electrode (SCE), CE - Counter-Electrode, WE - Working Electrode (specimen area 1.936 cm^2).

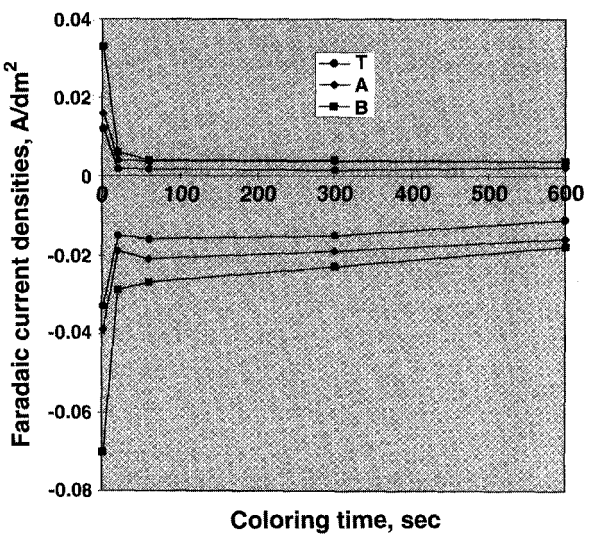

Fig. 2—Anodic and cathodic faradaic current densities at 1 and 20 sec, 1, 5 and 10 min of electrolytic coloring of anodized aluminum samples in solutions T, A and B.